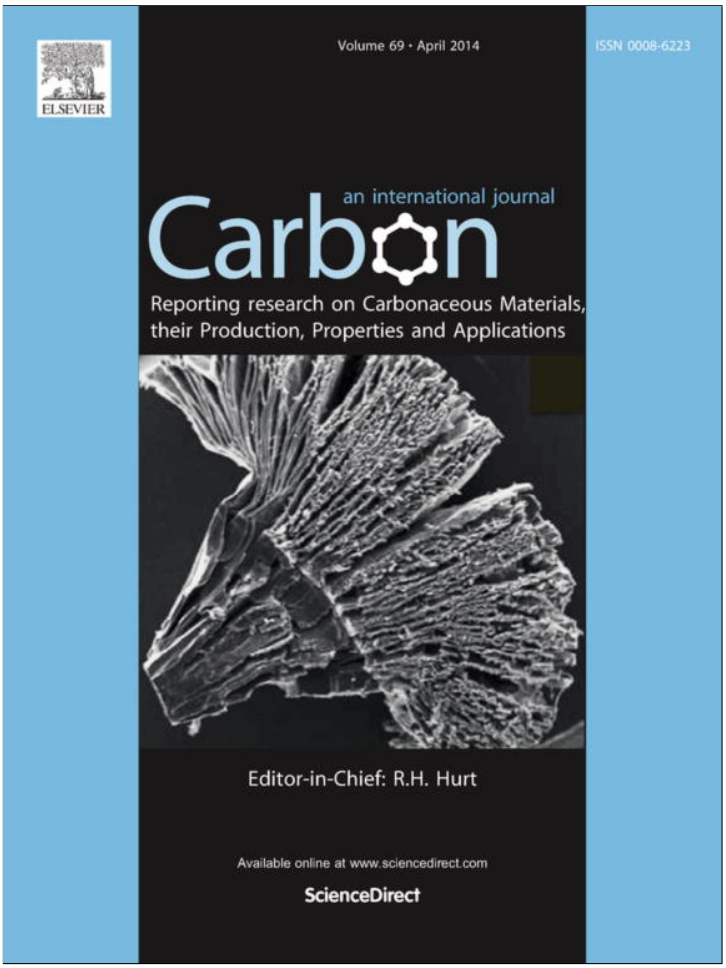

CARBON 69 (2014) 355–360

Available at www.sciencedirect.com

ScienceDirect

journal homepage: www.elsevier.com/locate/carbon

Density-functional tight-binding study of the collapse of carbon nanotubes under hydrostatic pressure

Tiago F.T. Cerqueira, Silvana Botti, Alfonso San-Miguel, Miguel A.L. Marques *

Institut Lumière Matière, UMR5306 Université Lyon 1-CNRS, Université de Lyon, F-69622 Villeurbanne Cedex, France

ARTICLE INFO

Article history:
Received 17 September 2013
Accepted 11 December 2013
Available online 17 December 2013

ABSTRACT

We investigate the radial collapse of carbon nanotubes bundles using the density-functional based tight-binding method for a large number of chiralities in the small diameter range. We find that for tubes larger than about 0.6 nm the collapse pressure fits a d^{-3} law, but with collapse pressures considerably larger than previous estimates based on classical potentials. Furthermore, we show that the effect of chirality on the collapse pressure is small, and that previous reports of large chiral effects are probably due to the use of too small unit cells. Our results are in good agreement with available experimental data, and provide a better understanding of the process of collapse of nanotubes under pressure.

1. Introduction

Since the outstanding paper by Iijima et al. [1] in 1991 carbon nanotubes remain an intense field of research. Their unique electronic and mechanical properties make them ideal candidates for novel electronics and new superhard materials. Despite their very high resilience and Young modules, it was observed that nanotubes can undergo ovalization and collapse, sometimes even at atmospheric pressure [2,3]. Unfortunately, the impact of these geometrical changes on the electronic properties is subject to debate [4–6]. Moreover, the collapse process itself is still not completely understood, as only indirect observation is reported. It is expected that the radial collapse pressure of a carbon nanotube is mainly determined by its diameter [7–12], but other factors, like the nanotube chirality, the presence of defects or the choice of the pressure transmitting medium, are also known to be relevant [13,14].

Experimentally, Raman spectroscopy is the main technique used to study the collapse of nanotube bundles. However there is not yet a clear consensus on the best spectroscopic signature of the collapse. Several footprints have been proposed: (i) the disappearance of the radial breathing mode signal, which has been used in literature either to identify the polygonization [15] or the ovalization [16] of the cross-section, or directly the tube collapse [17]; (ii) the change of slope [18,16,19], the presence of a plateau [17], or even the change of sign [20] of the curve representing the dependence of the G-band frequency with respect to pressure. However, the use of the progressive attenuation of the Raman modes intensity was questioned, due to the resonant character of the Raman signal [21], and the modifications of the resonance conditions induced by pressure [22,23]. Many factors, in fact, contribute to make the experimental results difficult to interpret: the inhomogeneity of the geometrical characteristics of the tubes in the samples, impurities and defects resulting from the growing processes, or the use of different pressure transmitting media [24–27], which could eventually become solid before the observation of the collapse or even penetrate the tubes if they are open [25]. In fact, for tubes of similar diameters, the experimental values of the collapse pressure of single-wall bundles can differ of

* *Corresponding author.*
E-mail addresses: tiago.cerqueira@universite-lyon.fr (T.F.T. Cerqueira), marques@tddft.org (M.A.L. Marques).
0008-6223/$ - see front matter
http://dx.doi.org/10.1016/j.carbon.2013.12.036

more than one order of magnitude, and have been shown to be extremely sensitive to the nature of the pressure transmitting media [20]. Other experimental methods have been used to observe the pressure induced cross-section modifications, such as neutron diffraction [28] (indicating a progressive polygonization), X-ray diffraction [29] (with no indication of collapse transition up to 10 GPa, in arc-discharge carbon nanotubes) or optical spectroscopy [30].

There are many theoretical papers dealing with the collapse of carbon nanotubes. Unfortunately, theoretical works using different methods and setups are known to give dissimilar and sometimes even contradictory results. In particular, calculations performed with classical potentials usually yield collapse pressures of around half the ones obtained with *ab initio* methods [11]. However, even when calculations are performed with comparable approaches, the output values for the collapse pressure are very scattered and difficult to reconcile. The reasons for this problem are easy to understand if we consider that calculations are usually performed using either classical potentials or density-functional theory. While the latter is certainly the most precise method, density-functional simulations are numerically very heavy, and therefore calculations are usually performed for very small unit cells containing only one (zigzag or armchair) nanotube. Classical potentials are certainly numerically much more efficient, and allow for simulations of unit-cells containing several nanotubes of diverse diameters and chiralities. However, they suffer from an intrinsic problem of precision: while designing classical potentials for either sp^2 or sp^3 carbon is relatively easy, nanotubes contain a combination of both bonds, a situation much more complicated to describe classically.

With this work we aim at clarifying the existing controversies by performing accurate simulations of a large number of single-wall nanotubes with a variety of diameters and chiralities, in several setups. In view of the problem of precision of classical potentials in this context, we chose to stick to a quantum–mechanical description. As the use of density-functional theory would limit considerably the size of the systems that we were able to study, we chose therefore a more efficient alternative, namely the density-functional based tight-binding method (DFTB) [31,32]. This approach can be seen as an approximation to the Kohn–Sham density-functional theory, where the usual integrals are fitted to reference calculations. This allows for faster simulations while keeping much better transferability and accuracy than other semi-empirical methods. This method is particularly good for carbon compounds as demonstrated in previous works [31,33–35]. Since carbon nanotubes are relatively inert structures where no significant charge transfer is expected [33], we decided to adopt the non-self-consistent charge scheme of DFTB. It is true that there is a small charge transfer *after* the collapse as a result of the modified curvature [40], but this is not expected to affect the pressure at which the collapse takes place.

2. Method

We performed quasi-static DFTB calculations on 69 single-wall carbon nanotubes bundles using the DFTB+ software package [36] (with the matsci-0–3 parameters set [37]). Even if this form of tight-biding has already been extensively tested, we performed a simple validation test of our setup, by comparing the lattice constant of the (10, 10) nanotube at ambient pressure (1.69 nm) with the experimental [38] (1.70 nm) and DFT values [39] (1.65 – 1.69 nm, depending on the exchange and correlation functional and pseudo-potential used). The DFTB value is in very good agreement with both.

The set of systems under study includes basically all nanotubes with less than 300 atoms in the unit cell and with diameters up to 1.9 nm. Our simulations were performed using hexagonal unit cells containing 1, 2 and 4 nanotubes with periodic boundary conditions in the three directions. (For unit cells containing 4 tubes we included only nanotubes with less than 150 atoms due to the increased computation requirements.) A minimum tube length of 1.98 nm was assured in all cases, which corresponds to four primitive unit cells for the armchair nanotubes. The initial distance between the nanotubes in the bundle was set to 0.335 nm.

For each value of pressure, a random displacement of 0.002 nm, was applied on each atom. After that, geometry and cell vectors were optimized until all the forces became smaller than 10^{-4} Ha/Bohr. The applied pressure was increased in steps of 0.2 GPa up to 30 GPa or until collapse. The collapse of the tubes is abrupt in the large majority of the cases and it was identified by a discontinuity in the Gibbs Energy, that corresponds to the transformation to a peanut-like geometry. In some rare cases this discontinuity was not found and the collapse pressure was determined by inspection, *i.e.*, we assigned the collapse to the first peanut-like geometry found.

3. Results and discussion

We start by analyzing how the number of tubes in the unit cell influences the collapse pressures. It is evident that having only one tube per unit cell is a large constraint, allowing only symmetric collapses, while having more tubes opens up other possible collapse channels (see Fig. 1). To estimate how this influences the collapse pressure, we performed simulations using 1, 2, and 4 nanotubes per unit cell and maintaining equal all other parameters of the simulation. Fig. 2 summarizes our results for tubes containing less than 150 atoms. The two lines represent fits of the data for tubes larger than 0.6 nm diameter with the function

$$P_{\text{collapse}} = \alpha/(\beta + D)^3, \quad (1)$$

where D is the diameter. Fig. 2 shows that using 2 or 4 tubes per cell yields similar results, but having only one tube per cell leads to a much larger dispersion of the collapse pressures. This clearly proves that one tube per cell is not enough to describe correctly the bundle interactions. A recent theoretical work [14] concluded that, for a comparable diameter of about 1.35 nm, the collapse pressure of an armchair single-wall carbon nanotube is several (13.75) times higher than the one of a zigzag nanotube. Our accurate calculations suggest that that result is likely to be an artifact of using only one tube in the unit cell. In particular, for (10, 10) and (17, 0) CNTs, our simulations yield collapse pressures of 3.4 and 3.6 GPa, to compare with the values reported in Ref.

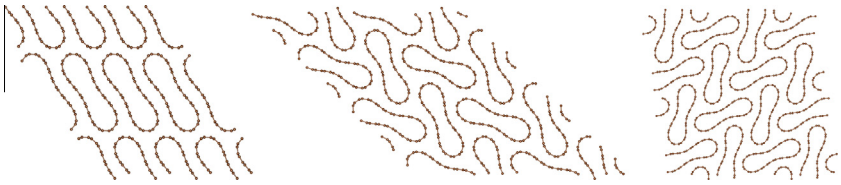

Fig. 1 – Collapsed bundle of (10,10) nanotubes in the case of 1 tube per cell (left), 2 tubes per cell (center) and 4 tubes per cell (right). (A colour version of this figure can be viewed online.)

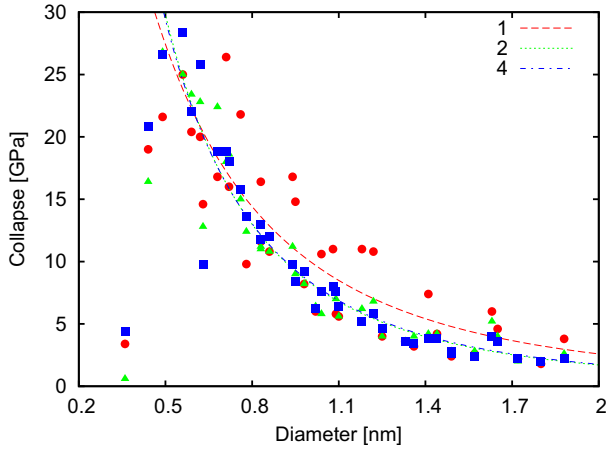

Fig. 2 – Collapse pressure as a function of the nanotube diameter for 1 (circles), 2 (triangles) and 4 (squares) nanotubes in the unit cell. The lines are fits to with Eq. 1. (A colour version of this figure can be viewed online.)

[14] of ~ 5.5 and ~ 0.4 GPa, respectively. The choice of using one tube per unit cell might be one of the reasons for the observed discrepancies in the results published in the literature.

As we proved that the differences between having 2 and 4 tubes are not significant (see Fig. 3), we will focus the rest of the discussion on the case of 2 tubes per unit cell for which we have results for more chiralities. The solid black line in Fig. 3 is again a fit using Eq. 1 (yielding $\alpha = 24.6$ GPa nm^3 and $\beta = 0.4$ nm, while the dashed line reproduces the results of Ref. [7]). If we consider tubes with diameters above 0.6 nm, we find an overall good agreement with the well known D^{-3} behavior. However, below this value, the collapse pressures start to decrease with decreasing diameter. This is related to the increased curvature of the graphene sheet that causes higher load on the C–C bonds. For small tubes, we even see for some chiralities the formation of interlinked sp^3 structures connecting adjacent nanotubes after collapse. For really small nanotubes, such as the (5,0) and (7,0), these interlinked structures are already present at ambient pressure. The existence of these structures has been reported experimentally [41] and theoretically [42,39,43].

Quantitatively, we obtained collapse pressures that are roughly the double of the majority of other theoretical works based on classical potentials [7] (see Fig. 3). For nanotube diameters in the range of 1.2 to 1.5 nm, which typically correspond to arc-discharge synthesized carbon nanotube bundles, our calculated collapse pressures range from 3 to 7 GPa. As already explained, the experimental values proposed for the collapse pressures are highly spread. Considering the case of arc-discharge bundles and only the case of studies using either 4:1 methanol:ethanol or argon as pressure transmitting medium, which exhibit good hydrostatic conditions up to 10 GPa, phase transformations towards collapsed forms were reported at 10 GPa using Raman spectroscopy [18,25] or X-ray diffraction [29]. Other works [41] report the collapse of arc-discharge bundles at pressures of 5 GPa. Our calculated values in the 3–7 GPa interval

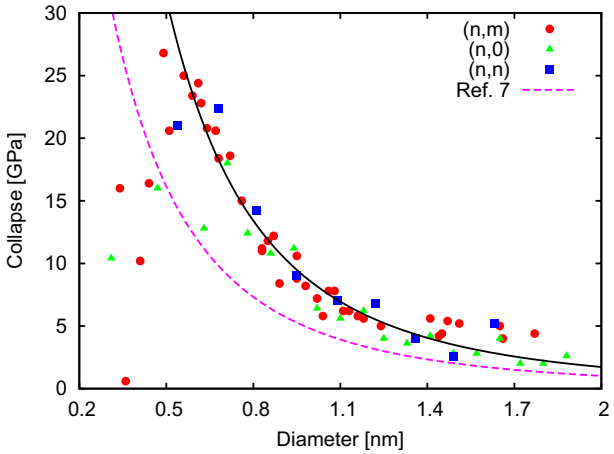

Fig. 3 – Collapse pressure as a function for zig-zag, armchair and chiral nanotubes diameter, using 2 CNTs per unit cell. (A colour version of this figure can be viewed online.)

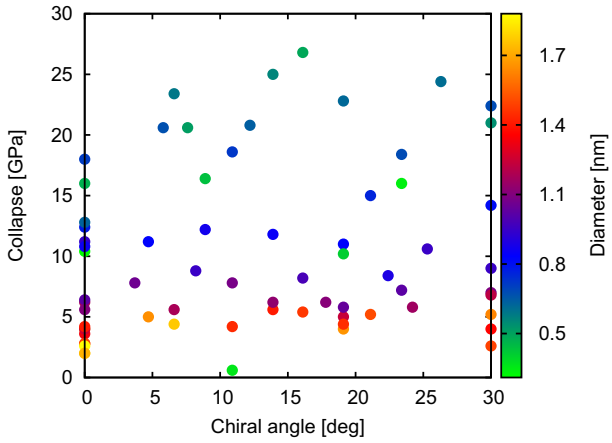

Fig. 4 – Collapse pressure as a function of the chiral angle calculated with two tubes per unit cell. The nanotube diameter is indicated by the color scale. (A colour version of this figure can be viewed online.)

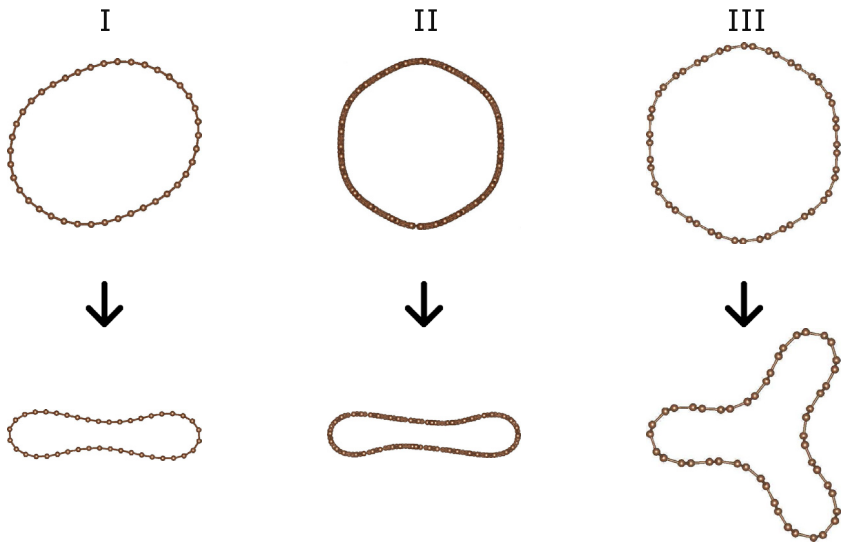

Fig. 5 – Collapse modes observed. From the top: Mode I, from ovalized to peanut geometry; Mode II, from polygonized to peanut; Mode III, from polygonized to star. (A colour version of this figure can be viewed online.)

compare very well with the experimental values ranging from 5 to 10 GPa for arc-discharge carbon nanotube bundles.

In order to study the effects of chirality on the collapse, we plotted the collapsed pressure as a function of the chiral angle in Fig. 4 in the case of two tubes per unit cell. The diameter is represented by the color scale on the right. For the smallest nanotubes chirality has a large influence in the collapse pressure, which can be understood as a consequence of the lower number of carbon atoms forming the nanotube wall, resulting in less cylindrical (more polygnized) nanotubes. For larger nanotubes no correlation between the chirality and the collapse pressure is noticeable.

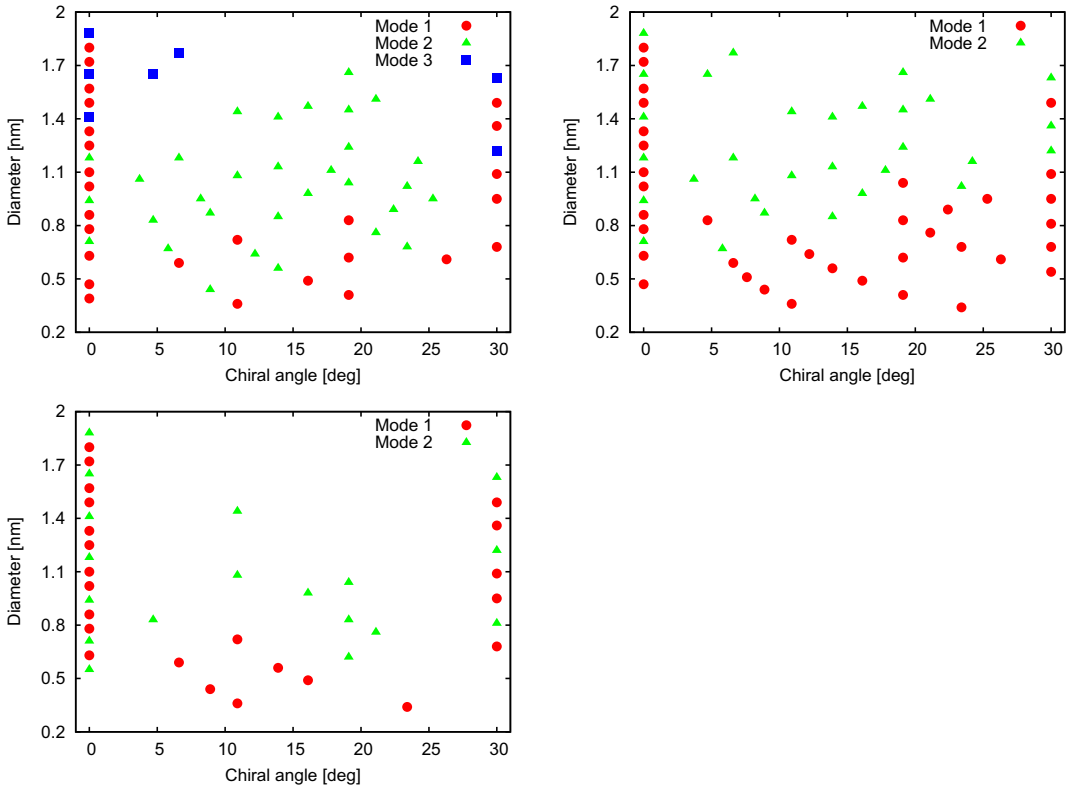

Fig. 6 – Collapse mode as a function of the diameter and the chiral angle of the nanotube. The top panel is for 1 tube per unit cell, the middle panel for 2 tubes per cell, and the bottom panel for 4 tubes per cell. (A colour version of this figure can be viewed online.)

Finally, we inspected the different possible collapse channels. We found three possibilities, as shown Fig. 5: mode I represents the transformation from ovalized to peanut, mode II the transformation from hexagonal to peanut and mode III from hexagonal to a star-like geometry. Fig. 6 displays the collapse mode as function of the chiral angle and the nanotube diameter for unit cells containing 1, 2 and 4 tubes. The collapse mode depends slightly on the number of tubes in the unit cell used, and it depends strongly on the diameter and the chirality. As it was already noted by other authors [39], armchair nanotubes with chiral vectors $(3n+3, 3n+3)$ adopt a polygonized structure before collapse, whereas the remaining nanotubes collapse from an ovalized structure. Interestingly, zigzag nanotubes with chiral vectors $(3n+3, 0)$ seem to collapse also going through a polygonal geometry. For other nanotubes, the collapse mode seems to be controlled by the diameter: small nanotubes ovalize and large one polygonize. Evidences of polygonalized CNTs where also reported experimentally [44] for nanotubes with diameters around 1.7 nm.

With only one nanotube per unit cell, we observed in some cases the collapse to an unusual star-like structure. This structure was predicted to be a possible collapse mode [45], although with a higher binding energy than the peanut geometry. We also notice that the pressure range of polygonization is smaller than the one of ovalization.

It was shown in classical simulations [46,13,47] that the energetically most favourable arrangement of collapsed nanotubes is the one with parallel nanotubes. This was also seen in high-resolution transmission electron microscopy (HRTEM) experiments on collapsed double-wall bundles with large diameters [48]. Indeed, it is plausible that for very large diameters the most stable collapsed structure consists of parallel nanotubes, as this geometry maximizes the van der Waals interaction between the walls. However, for smaller tubes, it is also clear [49,13] that other factors, such as the number of tubes in the simulation cell, the filling factor of the collapsed tubes, the environment, etc., may have a big influence on the collapsed geometry. In our simulations, the parallel geometry appeared for several bundles, while there were other cases where the herringbone geometry was found instead. We note, however, that the DFTB method does not describe accurately van der Walls interactions. Even if this contribution is small, it is of the order of the energy difference between the herringbone and the parallel arrangements ($\approx$ 10 meV per atom) and can therefore change the energetic ordering of the structures.

4. Conclusions

We studied the collapse of carbon nanotubes bundles under hydrostatic pressure for a wide range of diameters and chiralities using the density-functional based tight-binding method. Concerning the calculated collapse pressures, we show that the discrepancies found in the literature can be explained by the different number of carbon nanotubes in the unit cell and by the theoretical framework employed. Furthermore, using a quantum–mechanical approach, we obtained collapse pressures that are about twice as large as the ones obtained with classical potentials. The chirality of the nanotube does not show a strong influence on the collapse pressure for nanotubes bundles with diameters above 1 nm but it can be significant for smaller diameters. Finally, we obtain that the carbon nanotubes with diameters of around 0.6 nm are the ones with the highest collapse pressures.

Regarding the collapse modes, armchair and zigzag nanotubes polygonize before collapsing to a peanut geometry if their chirality equals $(3n+3, 3n+3)$ or $(3n+3, 0)$, whereas in the other cases the nanotubes adopt oval cross sections before collapsing. For chiral nanotubes, the collapse mode seems to be independent of the chiral angle, being the diameter the underlying factor.

We can conclude from our results that there are two key ingredients that are mandatory to perform quantitative simulations of the collapse process of carbon nanotubes under pressure: (i) a quantum mechanical description and (ii) large unit cells containing several tubes. In our opinion all previous literature on the subject should be critically reviewed based on this consideration.

Acknowledgments

The authors acknowledge financial support from the French ANR 2011 NANO 025 (TRI-CO). Computational resources were provided by GENCI (project x2012096017).

REFERENCES

[1] Iijima S et al. Helical microtubules of graphitic carbon. Nature 1991;354(6348):56–8.
[2] Chopra NG, Benedict LX, Crespi VH, Cohen ML, Louie SG, Zettl A. Fully collapsed carbon nanotubes. Nature 1995;377(6545):135–8.
[3] Motta M, Moisala A, Kinloch I, Windle A. High performance fibres from dog bone carbon nanotubes. Adv Mater 2007;19(21):3721–6.
[4] Chen D, Sasaki T, Tang J, Qin LC. Effects of deformation on the electronic structure of a single-walled carbon nanotube bundle. Phys Rev B 2008;77:125412.
[5] Nishidate K, Hasegawa M. Universal band gap modulation by radial deformation in semiconductor single-walled carbon nanotubes. Phys Rev B 2008;78:195403.
[6] Nishidate K, Hasegawa M. Deformation and transfer doping of a single-walled carbon nanotube adsorbed on metallic substrates. Phys Rev B 2010;81:125414.
[7] Elliott JA, Sandler JKW, Windle AH, Young RJ, Shaffer MSP. Collapse of single-wall carbon nanotubes is diameter dependent. Phys Rev Lett 2004;92(0955):095501.
[8] Pugno NM, Elliott JA. Buckling of peapods, fullerenes and nanotubes. Physica E 2012;44:944–8.
[9] Gadagkar V, Maiti PK, Lansac Y, Jagota A, Sood AK. Collapse of double-walled carbon nanotube bundles under hydrostatic pressure. Phys Rev B 2006;73:085402.
[10] Yang X, Wu G, Dong J. Structural transformations of double-walled carbon nanotube bundle under hydrostatic pressure. Appl Phys Lett 2006;89(11):113101 (pages 3).
[11] Sun DY, Shu DJ, Ji M, Liu F, Wang M, Gong XG. Pressure-induced hard-to-soft transition of a single carbon nanotube. Phys Rev B 2004;70:165417.
[12] Capaz RB, Spataru CD, Tangney P, Cohen ML, Louie SG. Hydrostatic pressure effects on the structural and electronic properties of carbon nanotubes. Phys Status Solidi B 2004;241(14):3352–9.

[13] Shanavas KV, Sharma SM. Molecular dynamics simulations of phase transitions in argon-filled single-walled carbon nanotube bundles under high pressure. Phys Rev B 2009;79:155425.

[14] Ling CC, Xue QZ, Chu LY, Jing NN, Zhou XY. Radial collapse of carbon nanotubes without and with stone-wales defects under hydrostatic pressure. RSC Adv 2012;2:12182–9.

[15] Venkateswaran UD, Rao AM, Richter E, Menon M, Rinzler A, Smalley RE, et al. Probing the single-wall carbon nanotube bundle: Raman scattering under high pressure. Phys Rev B 1999;59:10928–34.

[16] Peters MJ, McNeil LE, Lu JP, Kahn D. Structural phase transition in carbon nanotube bundles under pressure. Phys Rev B 2000;61:5939–44.

[17] Yao M, Wang Z, Liu B, Zou Y, Yu S, Lin W, et al. Raman signature to identify the structural transition of single-wall carbon nanotubes under high pressure. Phys Rev B 2008;78:205411.

[18] Sood AK, Teresdesai PV, Muthu DVS, Sen R, Govindaraj A, Rao CNR. Pressure behaviour of single wall carbon nanotube bundles and fullerenes: a Raman study. Phys Status Solidi B 1999;215(1):393–401.

[19] Sandler J, Shaffer MSP, Windle AH, Halsall MP, Montes-Morán MA, Cooper CA, et al. Variations in the Raman peak shift as a function of hydrostatic pressure for various carbon nanostructures: a simple geometric effect. Phys Rev B 2003;67:035417.

[20] Caillier C, Machon D, San-Miguel A, Arenal R, Montagnac G, Cardon H, et al. Probing high-pressure properties of single-wall carbon nanotubes through fullerene encapsulation. Phys Rev B 2008;77:125418.

[21] Merlen A, Bendiab N, Toulemonde P, Aouizerat A, San Miguel A, Sauvajol JL, et al. Resonant Raman spectroscopy of single-wall carbon nanotubes under pressure. Phys Rev B 2005;72:035409.

[22] Ghandour AJ, Dunstan DJ, Sapelkin A, Proctor JE, Halsall MP. High-pressure Raman response of single-walled carbon nanotubes: effect of the excitation laser energy. Phys Rev B 2008;78:125420.

[23] Ghandour AJ, Dunstan DJ, Sapelkin A. G-mode behaviour of closed ended single wall carbon nanotubes under pressure. Phys Status Solidi B 2009;246(3):491–5.

[24] Kawasaki S, Matsuoka Y, Yokomae T, Nojima Y, Okino F, Touhara H, et al. Effect of a liquid pressure-transmitting medium on the high pressure behavior of open- and closed-end single-walled carbon nanotubes and of c60-peapods. Phys Status Solidi B 2004;241(15):3512–6.

[25] Merlen A, Toulemonde P, Bendiab N, Aouizerat A, Sauvajol JL, Montagnac G, et al. Raman spectroscopy of open-ended single wall carbon nanotubes under pressure: effect of the pressure transmitting medium. Phys Status Solidi B 2006;243(3):690–9.

[26] Proctor JE, Halsall MP, Ghandour A, Dunstan DJ. Raman spectroscopy of single-walled carbon nanotubes at high pressure: effect of interactions between the nanotubes and pressure transmitting media. Phys Status Solidi B 2007;244(1):147–50.

[27] Gao K, Dai R, Zhao Z, Zhang Z, Ding Z. Effects of pressure transmitting media on Raman features of single-walled carbon nanotubes. Solid State Commun 2008;147(1–2):65–8.

[28] Rols S, Goncharenko IN, Almairac R, Sauvajol JL, Mirebeau I. Polygonization of single-wall carbon nanotube bundles under high pressure. Phys Rev B 2001;64:153401.

[29] Sharma SM, Karmakar S, Sikka SK, Teredesai PV, Sood AK, Govindaraj A, et al. Pressure-induced phase transformation and structural resilience of single-wall carbon nanotube bundles. Phys Rev B 2001;63:205417.

[30] Anis B, Haubner K, Börrnert F, Dunsch L, Rümmeli MH, Kuntscher CA. Stabilization of carbon nanotubes by filling with inner tubes: an optical spectroscopy study on double-walled carbon nanotubes under hydrostatic pressure. Phys Rev B 2012;86:155454.

[31] Porezag D, Frauenheim T, Köhler T, Seifert G, Kaschner R. Construction of tight-binding-like potentials on the basis of density-functional theory: application to carbon. Phys Rev B 1995;51:12947–57.

[32] Seifert G, Porezag D, Frauenheim T. Calculations of molecules, clusters, and solids with a simplified lcao-dft-lda scheme. Int J Quantum Chem 1996;58(2):185–92.

[33] Zheng G, Irle S, Morokuma K. Performance of the dftb method in comparison to dft and semiempirical methods for geometries and energies of c20–c60 fullerene isomers. Chem Phys Lett 2005;412(1–3):210–6.

[34] Malola S, Häkkinen H, Koskinen P. Raman spectra of single-walled carbon nanotubes with vacancies. Phys Rev B 2008;77:155412.

[35] Botti S, Amsler M, Flores-Livas JA, Ceria P, Goedecker S, Marques MAL. Carbon structures and defect planes in diamond at high pressure. Phys Rev B 2013;88:014102.

[36] Aradi B, Hourahine B, Frauenheim T. Dftb+, a sparse matrix-based implementation of the dftb method. J Phys Chem A 2007;111(26):5678–84.

[37] Frenzel J, Oliveira AF, Jardillier N, Heine T, Seifert G. Semi-relativistic, self-consistent charge slater-koster tables for density-functional based tight-binding (dftb) for materials science simulations. 2004–2009. http://www.dftb.org/parameters/download/matsci/matsci_0_3/.

[38] Thess A, Lee R, Nikolaev P, Dai H, Petit P, Robert J, et al. Crystalline ropes of metallic carbon nanotubes. Science 1996;273(5274):483–7.

[39] Saxena S, Tyson TA. Interacting quasi-two-dimensional sheets of interlinked carbon nanotubes: a high-pressure phase of carbon. ACS Nano 2010;4(6):3515–21.

[40] Shklyaev OE, Mockensturm E, Crespi VH. Modeling electrostatically induced collapse transitions in carbon nanotubes. Phys Rev Lett 2011;106:155501.

[41] Lu S, Yao M, Li Q, lv H, Liu D, Liu B, et al. Exploring the possible interlinked structures in single-wall carbon nanotubes under pressure by Raman spectroscopy. J Raman Spectrosc 2013;44(2):176–82.

[42] Cheng H, Pez GP, Cooper AC. Spontaneous cross linking of small-diameter single-walled carbon nanotubes. Nano Lett 2003;3(5):585–7.

[43] Reich S, Thomsen C, Ordejón P. Elastic properties and pressure-induced phase transitions of single-walled carbon nanotubes. Phys Status Solidi B 2003;235(2):354–9.

[44] López MJ, Rubio A, Alonso JA, Qin LC, Iijima S. Novel polygonized single-wall carbon nanotube bundles. Phys Rev Lett 2001;86:3056–9.

[45] Zang J, Treibergs A, Han Y, Liu F. Geometric constant defining shape transitions of carbon nanotubes under pressure. Phys Rev Lett 2004;92:105501.

[46] Zhang XH, Liu ZF, Gong XG. Comment on collapse of single-wall carbon nanotubes is diameter dependent. Phys Rev Lett 2004;93:149601.

[47] Yang X, Wu G, Zhou J, Dong J. Single-walled carbon nanotube bundle under hydrostatic pressure studied by first-principles calculations. Phys Rev B 2006;73(2354):03.

[48] Zhong XH, Wang R, Liu LB, Kang M, Wen YY, Hou F, et al. Structures and characterizations of bundles of collapsed double-walled carbon nanotubes. Nanotechnology 2012;23(50):505712.

[49] Elliott JA, Sandler JKW, Windle AH, Young RJ, Shaffer MSP, Elliott, et al. Phys Rev Lett 2004;93:149602. reply.